JOURNAL OF MATERIALS SCIENCE **35** (2000) 391 – 397

Characterization of coated particulate fillers

M. GILBERT
Institute of Polymer Technology and Materials Engineering, Loughborough University, UK

I. SUTHERLAND
Department of Chemistry, Loughborough University, UK
E-mail: I.Sutherland@lboro.ac.uk

A. GUEST
Institute of Polymer Technology and Materials Engineering, Loughborough University, UK

Stearic acid coated samples of porous and non-porous grades of magnesium hydroxide and calcium carbonate have been characterized using diffuse reflectance infra red (DRIFT), and X-ray photoelectron spectroscopy (XPS). Using DRIFT, the signal due to the reacted coating reached a plateau at a coating level dependent on the filler surface area. XPS showed that coating thickness increased with the amount of coating, slope changes being observed in plots at lower levels of applied coating than those observed by DRIFT. The differences between the measurements for the two techniques is attributed to their different sampling depths. The FTIR having a greater sampling depth probes the internal surface area of the agglomerates present in the porous material, whereas XPS does not. The surface chemistry of the two types of coated filler is compared.

1. Introduction

The programme described here, focuses on the process of filler coating, and the characterization of coated fillers. The effects of coatings on processing behaviour and product properties have also been studied.

Dry coating is a widely used and cheap method of coating the surface of fillers. It is a single step process and does not require drying of the filler after exposure to aqueous solutions. Despite the commercial importance of the process there appear to have been few published studies of the dry coating of particulate fillers. X-ray photoelectron spectroscopy (XPS) and diffuse reflectance infra red (DRIFT) techniques have been identified as appropriate for the characterization of filler/coating interaction [1] but their use so far for coatings on particulate fillers has been fairly limited. The latter technique was used to investigate the surface treatment of a variety of particulate fillers with silane surface coatings [2] and more recently for the study of surface modified aluminium hydroxide [3]. Fekete *et al.* [4] have used XPS to study the interaction between calcium carbonate and stearic acid, and have estimated coating thickness from the results produced. The use of both infra red spectroscopy and XPS for the analysis of silane treated talc has been reported [5].

In this work, the XPS and DRIFT results have been used combined to study the stearic acid coating of magnesium hydroxide, and these techniques have also been used to investigate further the coating of calcium carbonate with stearic acid.

2. Experimental

2.1. Filler coating

The fillers studied in detail were two ICI development grades of magnesium hydroxide, one containing porous, and one containing non-porous particles. Their surface areas are listed in Table I, and SEM photographs of the two magnesium hydroxides are shown in Fig. 1. The porous grade is precipitated from sea water, and consists of tiny crystallites which cluster together to form aggregates, so that much of the surface area is internal. The non-porous grade magnesium hydroxide was produced by recrystallization of the first grade to produce crystals of controlled size and shape.

The two fillers were coated using up to 14% by weight of stearic acid.

The magnesium hydroxides were coated using a Waring laboratory scale mixer; 100 g filler/stearic acid mixes were heated gradually (over a period of 24 min) to 113 °C using a rotor speed of 7000 rpm. To investigate the applicability of the analysis methods to other systems, a commercial calcium carbonate was also examined. The calcium carbonate samples were coated with stearic acid at ECC using a Cowlishaw mixer of similar size to the Fielder. The charge was 1000 g and the rotor speed was 3000 rpm; heating was carried out for 15 min to a temperature of 90 °C.

2.2. DRIFT analysis

Filler coatings were analysed using a Nicolet 20DXC Fourier Transform Infra Red spectrometer with a

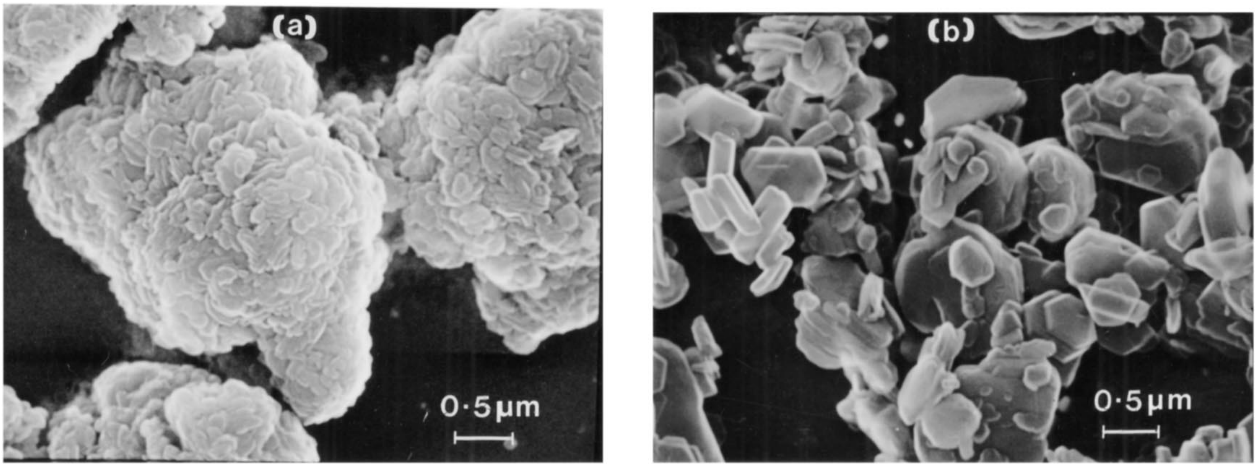

Figure 1 Scanning electron micrographs of magnesium hydroxide samples. (a) Porous; (b) non-porous.

TABLE I Surface areas of fillers[a]

Filler	Surface area ($m^2\ g^{-1}$)
Magnesium hydroxide (non-porous)	4.7
Magnesium hydroxide (porous)	13.2
Calcium carbonate (Polcarb 60)	3.3

[a] Measured by BET method.

diffuse reflectance accessory. The diffuse reflectance technique (DRIFT) was used to obtain quantitative assessment of the coatings. One part of coated filler was diluted with four parts of finely ground KBr in order to obtain the DRIFT spectra. Spectra were analysed to give quantitative data concerning coating levels.

2.3. X-ray photoelectron spectroscopy (XPS)

XPS spectra were recorded on VG ESCALAB spectrometer using AlK_α radiation. The spectra were quantified by measurement of peak area following subtraction of a Shirley type background. Correction was made for photoelectron cross-section [6], angular asymmetry parameter [7] energy dependence of the inelastic mean free path [8] and the transmission of the energy analyser [9]. Time under the X-ray beam was minimised and no significant beam damage observed. Samples were placed in a tray to a depth of about 2 mm. Photoelectrons were collected at 90° to the plane of the sample. The overall area analysed was approximately 0.5 cm^2, providing an average surface composition.

Assuming that a surface coating is uniform then the thickness of that coating may be estimated, for a flat surface, from the relative intensity of photoelectron peaks characteristic of substance and over layer respectively. In the calculation of thickness we have taken the density of the coating to be equal to that of stearic acid (0.94 g cm^{-3}) and the density of magnesium hydroxide to be 3.0 g cm^{-3}. Inelastic mean free paths in substrate and overlayer were estimated using semiempirical equations [8], the coatings being organic and the substrate inorganic. For analysis of magnesium hydroxide carbon 1s and magnesium 2p peaks were used. Assumption of a flat surface will tend to mean that the values obtained are if anything an over-estimate of the true values [10] for a uniform coating. *When photoelectrons are collected from a particulate filler there are a full range of take-off angles present. This has been the subject of detailed analysis [10]. The shallow take-off angles, around the diameter of the particle in the plane normal to the direction of photoemission, are not taken into account if a simple flat model is used to estimate coating thickness. If the particles are coated then the photoelectrons are forced to take a longer path through the the coating at shallow angles. The error introduced is substantial. Neglecting the difference in attenuation length between coating and substrate also introduces significant error.*

3. Results and discussion

3.1. Magnesium hydroxides

FTIR spectra from uncoated magnesium hydroxide, and for the same filler coated with 0.5% to 4.5% stearic acid are shown in Fig. 2. Various features can be observed. A group of peaks, centred at about 2900 cm^{-1}, due to symmetric and asymmetric CH_2 stretching, increases with increased coating level. The sharp band at 3697 cm^{-1} is due to the OH group in the magnesium hydroxide, but the absence of a carbonyl stretching band at about 1700 cm^{-1} showed that no unreacted stearic acid was detectable in any of the samples. A carboxylate band could be detected at 1570 cm^{-1}.

The stearic acid had therefore reacted with the filler surface according to the following equation:

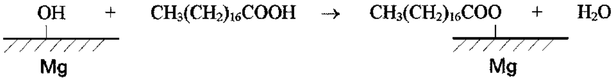

$$\underset{\text{Mg}}{\text{OH}} + CH_3(CH_2)_{16}COOH \rightarrow \underset{\text{Mg}}{CH_3(CH_2)_{16}COO} + H_2O$$

The area of the CH group of peaks was ratiod to that of the OH peak from the substrate, and plotted against coating level as shown in Fig. 3. It is seen that surface saturation occurs at a coating level of 3%. Similar results for the porous grade of magnesium hydroxide are shown in Fig. 4. Again a distinct slope change is seen at the same peak area ratio, but only when a coating level of 7–8% is reached, consistent with the greater surface area of this sample.

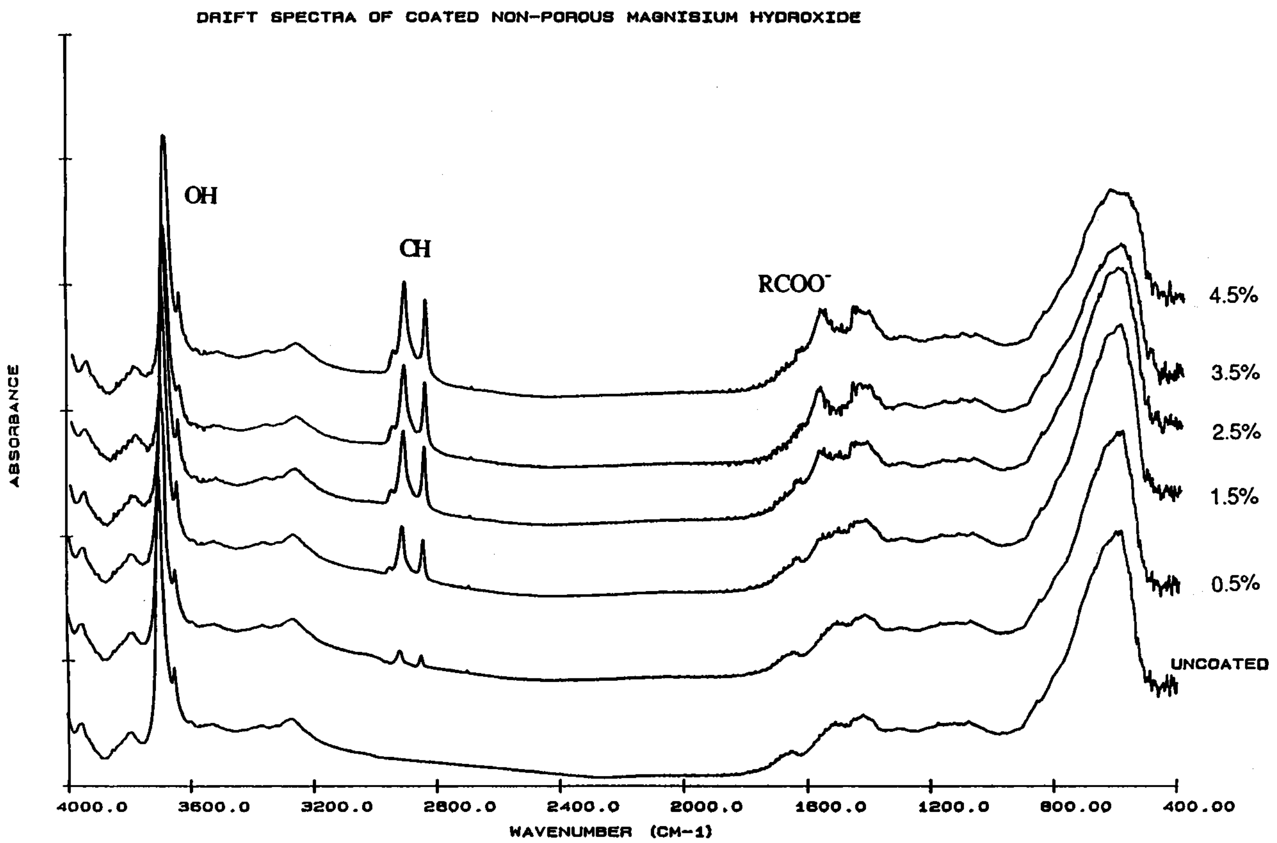

Figure 2 DRIFT spectra of coated non-porous magnesium hydroxide.

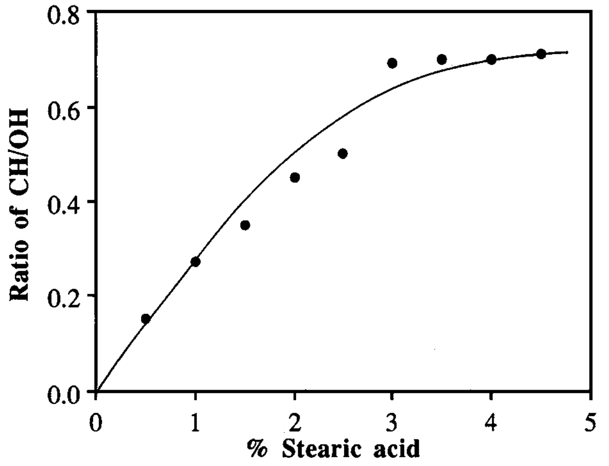

Figure 3 IR peak ratios for non-porous magnesium hydroxide coated with stearic acid.

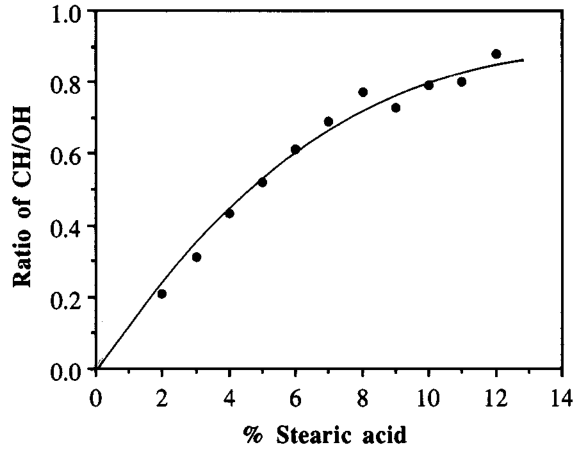

Figure 4 IR peak ratios for porous magnesium hydroxide coated with stearic acid.

More recent results to be reported later have shown that a plateau is not detected when coating is carried out to higher concentrations using a larger scale (8 litre) Fielder mixer. It is postulated that due to the high shear forces in the Waring the magnesium stearate produced by surface reaction is abraded and lost, with the result that a thicker surface coating is not built up. In the less severe conditions in the Fielder, loss of magnesium stearate does not occur so readily.

The effect of coating temperature is shown in Fig. 5. The non-porous magnesium hydroxide was coated with an excess (4%) of stearic acid, and the spectrum compared with that of a cold mix of coating and the filler. The CH_2 peaks were much weaker in the cold mix. It was seen that unreacted acid, physically mixed with the substrate, was not readily detectable using the DRIFT method. An almost identical result was obtained even when excess (15%) stearic acid was mixed with the porous magnesium hydroxide. (DRIFT is especially sensitive to organic coatings on reflective substrates since the IR will perform a double pass through the coating.)

X-ray photoelectron spectroscopy results for the porous grade of magnesium hydroxide are shown in Fig. 6. A progressive increase in the carbon 1s peak with increased coating weight is detected. XPS data were used to calculate coating thicknesses, assuming uniform coating, for both the porous and non-porous grades of magnesium hydroxide (Figs 7 and 8). The maximum thickness observed (~2.4 nm) corresponded

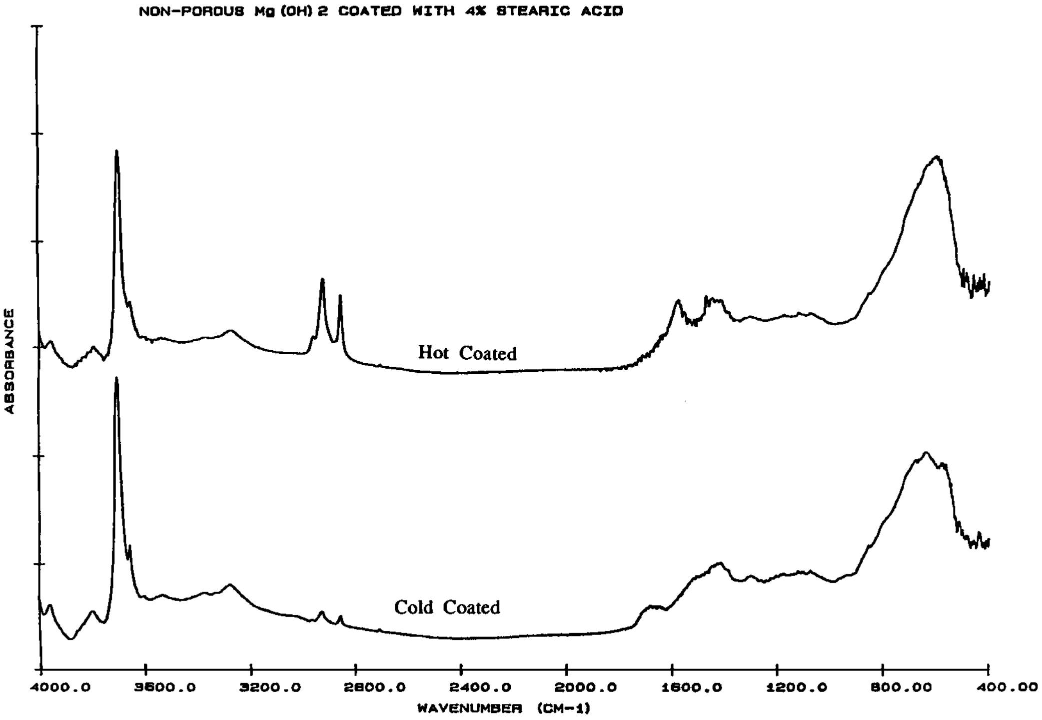

Figure 5 DRIFT spectra of non-porous magnesium hydroxide (a) using standard coating procedure; (b) after cold mixing.

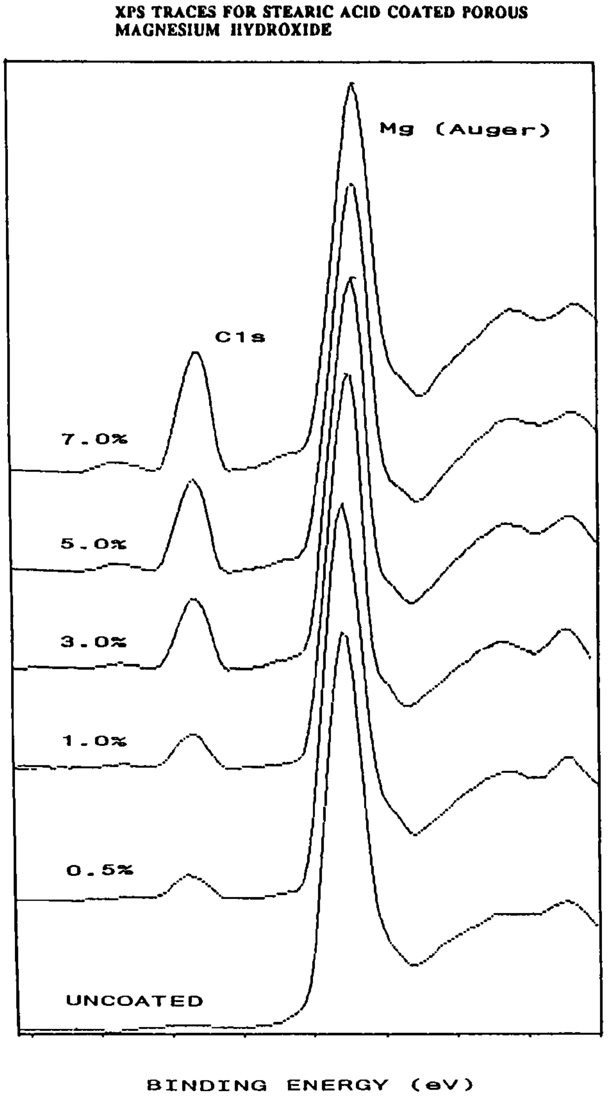

Figure 6 XPS traces for stearic acid coated porous magnesium hydroxide.

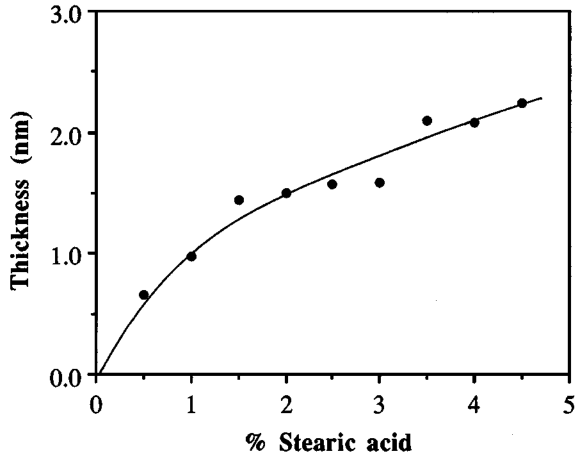

Figure 7 Coating thickness for porous magnesium hydroxide coated with stearic acid.

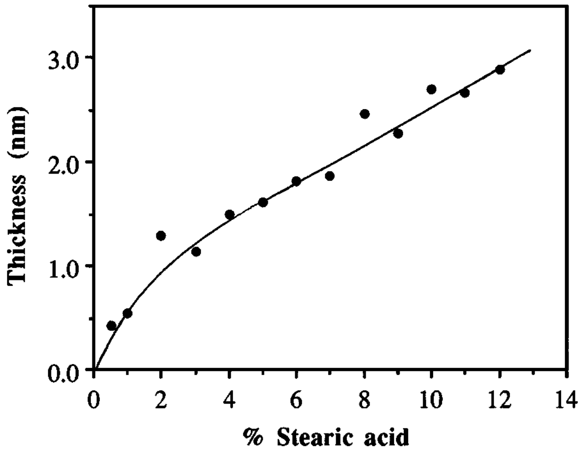

Figure 8 Coating thickness for non-porous magnesium hydroxide coated with stearic acid.

approximately to the length of a fully extended acid chain. The attenuation lengths for the photoelectrons involved depend on their kinetic energy and whether they are moving in the bulk filler or coating. The attenuation lengths for all photoelectorns involved was in the range 2–4 nm [10]. Thickness increased with coating level, with a slope change being observed at about 1.2% for non-porous magnesium hydroxide. This inflexion is expected to correspond to the completion of one monomolecular layer on the surface of the filler. If all of the acid added went to uniformly coat the filler then an addition of 1.2% of acid to the non-porous filler would produce a coating thickness of 2.8 nm. This is higher than the value calculated from the simple XPS model which could be due to the fact that magnesium stearate is being lost from the surface by abrasion, which is consistent with the results reported for the Fielder mixer earlier in this section. Non-uniformity in coating would also lead to an underestimate in coating thicknesses.

For the porous filler, scanning electron microscopy (Fig. 1) shows that the particles consist of aggregates of individual platelets. XPS, with a sampling depth of 2–3 nm will only probe the outer surface of the aggregate, whereas infra red radiation will penetrate to a depth of several microns into the aggregates. Thickness against coating level plots from XPS measurements for the porous magnesium hydroxide show a change in slope at about 2% by weight of filler added. Since XPS only probes the outer few nanometers then this probably indicates complete coverage of the outermost surfaces of the aggregates has been achieved at this level of added acid. The changes in slope are seen at higher coating levels in the FTIR plots than the XPS data. This is because FTIR detects coating of the internal surface of the aggregates which occurs after the outer surface has reacted.

3.2. Calcium carbonate

The infra-red spectrum of calcium carbonate itself is more complex than that of magnesium hydroxide. The free carbonate anion belongs to the D_{3h} space group, and theory predicts that there will be three fundamental infra-red active bands in the spectra [11, 12]. The fundamental bands at 713 cm^{-1} (v_4) and 877 cm^{-1} (v_2) are assigned as the degenerate bend and out-of-plane bend respectively. The large vibrational band from 1350–1650 cm^{-1} (v_3) contains the fundamental degenerate stretching frequency at $\sim$1419 cm^{-1}.

The additional bands are accounted for in terms of combinations and overtones [13, 14]. The maxima at 2980, 2960(sh) and 2870 cm^{-1} are the first overtone ($2v_3$) bands derived from the fundamental stretching (v_3) vibration of the carbonate anions. The bands at 2580(sh) and 2520 cm^{-1} are due to (v_1 (1083 cm^{-1}) + v_3) combination bands. The maximum at 1790 cm^{-1} has been given a number of assignments, with the most plausible being a combination of ($v_1 + v_2$).

FTIR spectra for uncoated calcium carbonate and a series of coated samples are shown in Fig. 9. As with magnesium hydroxide, a group of alkyl CH peaks is detected in the coated samples. However this band is superimposed on an overtone band with the result that accurate measurement of the intensity of the CH band

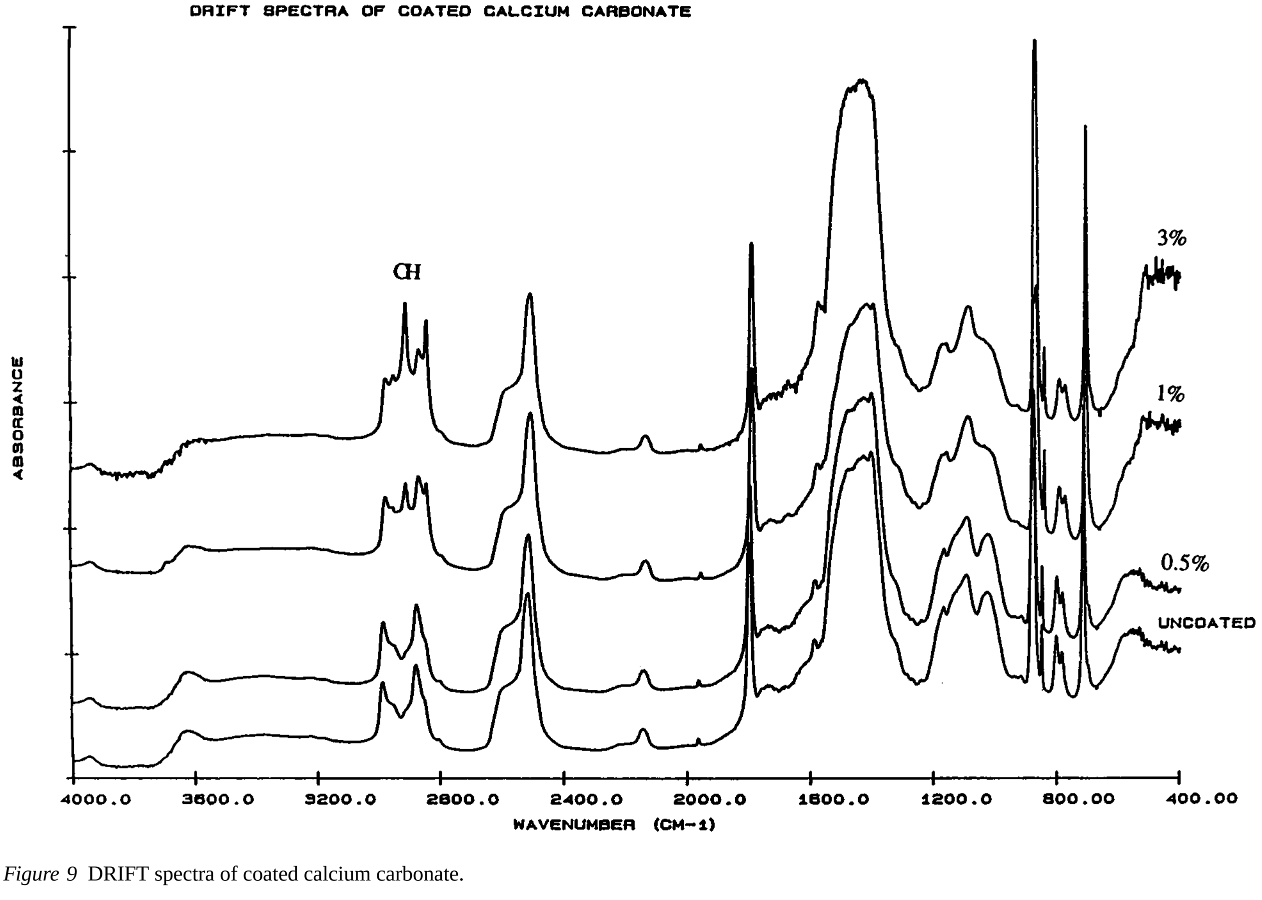

Figure 9 DRIFT spectra of coated calcium carbonate.

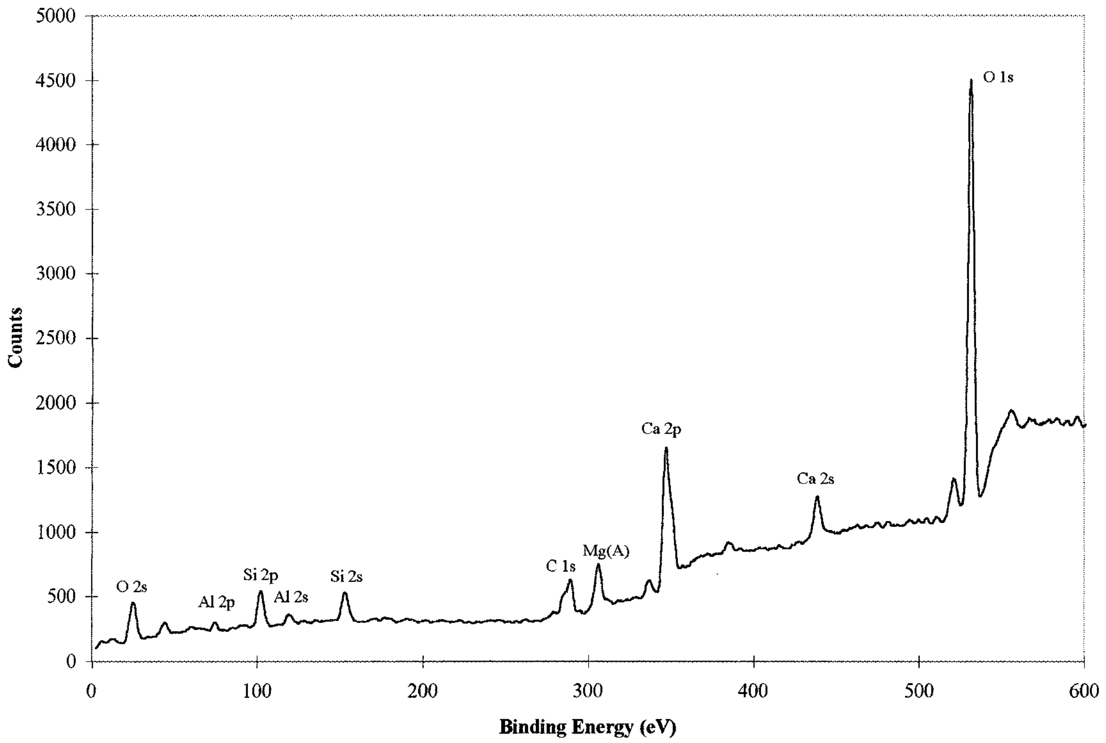

Figure 10 XPS trace for uncoated calcium carbonate.

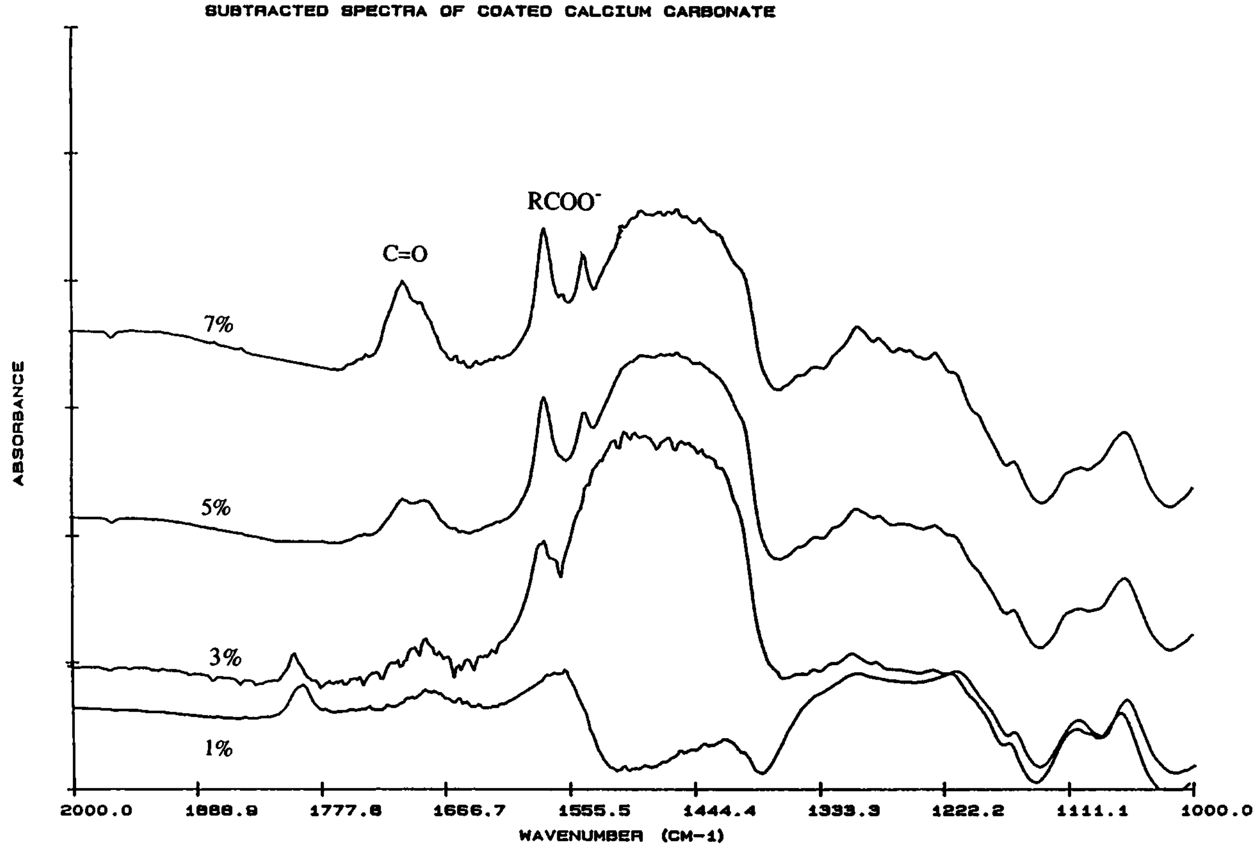

Figure 11 DRIFT spectra of coated calcium carbonate after subtraction of uncoated calcium carbonate.

is not easy without careful spectral subtraction. XPS spectra show that there is appreciable organic carbon (as distinct from carbonate) present on the surface of the filler prior to coating although this is not immediately obvious from inspection of the unsubtracted FTIR spectrum (Fig. 9). The broad scan XPS spectrum (Fig. 10) also shows appreciable amounts of silicon, suggesting the presence of silica/silicate. Clearly the interfacial chemistry here is a great deal more complex than was the case with the magnesium hydroxide.

The IR peaks due to $-COO^-$ are also masked, due to the strong absorbance at 1419 cm^{-1}. However, if the uncoated spectrum is subtracted from those of the coated fillers (Fig. 11), the $-COO^-$ bands at 1576 and 1540 cm^{-1} are then detectable. For the coated calcium carbonates, a C=O band at 1701 cm^{-1} due to free acid could be detected, its intensity increasing with % acid added. Results showed that in this case the stearic acid had partially reacted with the calcium carbonate surface to form stearate. XPS measurements indicate that the coating on the calcium carbonate is thicker than that on magnesium hydroxide, and this must be due in part to the presence of unreacted acid over the surface, and the presence of organic material on the surface prior to the coating. The existence of unreacted acid after coating calcium carbonate with stearic acid has also been reported by Fekete *et al.* [4]. The carbon 1s attenuation length in the coating is about 4 nm. Some of the carbonate is still visible making it impossible to reliably resolve acid groups. The presence of acid groups is however clearly resolved in the IR spectrum. The two techniques are thus complementary. It is interesting to note that although XPS is surface specific, FTIR is still more sensitive, and is better able to resolve the changes in surface chemistry of coated filler particles.

4. Conclusions

DRIFT can be used quantitatively to investigate the reaction between inorganic fillers and organic coatings. Using this technique, the organic molecules are more detectable after reaction with the filler. For the magnesium hydroxides studied, saturation coverage was detected at high concentrations by both DRIFT and XPS for the higher surface area porous filler. No unreacted stearic acid was detected even when very high coating concentrations were used.

For the non porous magnesium hydroxide, saturation is detected at a lower concentration using XPS than FTIR. It is suggested that this may relate to the relative penetration depth for the two techniques. Used in combination these two techniques can therefore follow the efficiency of coating for external and internal surface area of porous fillers.

IR studies of coated calcium carbonate were complicated by the presence of overtone bands of the stretching frequencies of the carbonate which obscures the CH stretching bands due to the coating. Surfaces may contain significant amounts of organic carbon which is not immediately obvious without careful spectral subtraction. Similar considerations also apply to detection of the stearate bands obscured by the carbonate stretching frequency at 1419 cm^{-1}. Unlike for magnesium hydroxide, unreacted acid is detected on the surface of the calcium carbonate filler as coating level increases.

Acknowledgements

Thanks are due to the Science and Engineering Research Council, ICI Chemicals and Polymers Ltd., European Vinyls Corporation (UK) Ltd., ECC International, Cookson Group plc, Stewarts and Lloyds Plastics and BP Chemicals International for support of the programme of which this work forms a part, and to Dr Carole Raymond and Dr Isla Mathieson for their assistance in obtaining the XPS spectra.

References

1. R. N. ROTHON, (ed.) "Particulate-Filled Polymer Composites" (Longman Scientific and Technical, Harlow, 1995).
2. H. ISHIDA and J. D. MILLER, "Composite Solutions to Material Challenges," Thirty Eighth Annual Conference Preprint, Houston, Texas, February 1983.
3. C. M. LIAUW, G. C. LEES, S. J. HURST, R. N. ROTHON and D. C. DOBSON, *Plast. Rubb. and Comp. Proc. and Appl.* **24** (1995) 211.
4. E. FEKETE, B. PÚKÁNSZKY, A. TÓTH and I. BERTÓTI, *J. Colloid and Interface Sci.* **135** (1990) 200.
5. A. ROUSSEAU, F. CLAUSS, R. BAEZA and Y. PIETRANSANTA, Conf. Proc. "Moffis 93," Namur, Belgium, April '93, p. 257.
6. J. H. SCOFIELD, *J. El Spec. Rel Ph.* **8** (1976) 129.
7. R. F. REILMAN, A. MSEGANE and S. T. MANSON, *ibid.* **8** (1976) 129.
8. M. P. SEAH and W. A. DENCH, *Surf. Int. Aral* **1** (1979) 2.
9. M. P. SEAH, *ibid.* **2** (1980) 222.
10. E. S. SHENG and I. SUTHERLAND, *Surface Science* **314** (1994) 325.
11. W. STERZEL and E. CHORINSKY, *Spectrochimica Acta* **24** (1968) 353–360.
12. W. NEAGLE and CH. ROCHESTER, *J. Chem. Soc. Faraday Trans.* **86** (1990) 181–183.
13. R. M. HEXTER *Spectrochimica Acta* **10** (1958) 281.
14. A. HOLMGREEN and W. FORSLING, *ibid.* **50** (1994) 1857–1869.

Received 17 June 1998
and accepted 15 June 1999